Biophysical Chemistry 150 (2010) 73–79

Contents lists available at ScienceDirect

Biophysical Chemistry

journal homepage: http://www.elsevier.com/locate/biophyschem

Suppression of IAPP fibrillation at anionic lipid membranes via IAPP-derived amyloid inhibitors and insulin

Daniel Sellin [a], Li-Mei Yan [b], Aphrodite Kapurniotu [b], Roland Winter [a,*]

[a] Physical Chemistry I - Biophysical Chemistry, Department of Chemistry, TU Dortmund University, Otto-Hahn Str. 6, D-44227, Dortmund, Germany
[b] Peptide Biochemistry, Center of Integrated Protein Science München, Technische Universität München, An der Saatzucht 5, D- 85354 Freising-Weihenstephan, Germany

ARTICLE INFO

Article history:
Received 11 December 2009
Received in revised form 20 January 2010
Accepted 21 January 2010
Available online 28 January 2010

Dedicated to Prof. Dr. Alfred Blume on the occasion of his 65th birthday.

Keywords:
ATR-FTIR spectroscopy
Protein aggregation
Amyloid
Lipid bilayer
Peptide inhibitors

ABSTRACT

Aggregation of human islet amyloid polypeptide (hIAPP) into cytotoxic β-sheet oligomers and amyloid plaques is considered a key event in pancreatic β-cell degeneration in type 2 diabetes (T2D). hIAPP is synthesized in the pancreatic β-cells and it is stored, co-processed in the secretory granules, and co-secreted to the extracellular matrix together with insulin. *In vivo*, hIAPP aggregation may start and proceed at the water-cell membrane interface and anionic lipid membranes strongly enhance the process of hIAPP fibrillization which is causally linked to membrane disintegration and cell degeneration. In this study we explored the amyloidogenic propensity and conformational properties of hIAPP in the presence of negatively charged membrane (DOPC/DOPG phospholipid bilayers) surfaces upon addition of two recently designed potent hIAPP-derived inhibitors of hIAPP amyloidogenesis, the hexapeptide NF(N-Me)GA(N-Me)IL (NFGAIL-GI) and the 37-residue non-amyloidogenic hIAPP analog [(N-Me)G24, (N-Me)I26]-IAPP (IAPP-GI). For comparison, the effects of insulin, which is a natively occurring hIAPP aggregation inhibitor, rat IAPP (rIAPP), which is a natively non-amyloidogenic hIAPP analog, and the hIAPP amyloid core peptide hIAPP(22-27) or NFGAIL were also studied. The aim of our study was to test whether and how the above peptides which have been shown to completely block or suppress hIAPP amyloidogenesis in bulk solution *in vitro* would also affect these processes in the presence of lipid membranes. To this end, attenuated total reflection Fourier-transform infrared spectroscopy (ATR-FTIR) was applied. We find that IAPP-GI, NFGAIL-GI, insulin, and rIAPP are potent inhibitors of hIAPP fibrillization. Importantly, our data also suggest that the hetero-complexes of IAPP-GI, rIAPP, and insulin with hIAPP although non-amyloidogenic *per se* are still able to adsorb at the lipid membrane. By contrast, in the presence of NFGAIL-GI, interaction of hIAPP with the lipid membrane is completely abolished, consistent with NFGAIL-GI mediated sequestration of hIAPP via hetero-complexation in the aqueous phase mainly accounting for the observed strong effect of NFGAIL-GI on hIAPP fibrillogenesis at the lipid membrane interface. Finally, our studies show that once hIAPP is fibrillized at the water-lipid membrane interface with fibrils being attached to the lipid membrane, it cannot be disaggregated by all above peptides.

1. Introduction

In the late stages of type II diabetes mellitus (T2DM), pancreatic β-cell death is accompanied by deposition of islet amyloid polypeptide (IAPP) amyloid fibers [1]. The human islet amyloid polypeptide (hIAPP), also known as amylin, is secreted by β-cells of the pancreas along with insulin [2]. Protein levels are maintained at a ~1:100 molar ratio of hIAPP to insulin in healthy β-cells, and levels of up to 1:20 are found in diseased cells [1–3]. hIAPP aggregation has been considered as the primary culprit for β-cell loss in T2DM patients. Normally, hIAPP, a largely disordered soluble 37-residue peptide, is believed to act as a neuroendocrine regulator of glucose homeostasis in a counterregulatory manner to insulin [1,2,4]. However, other than insulin [5], hIAPP is able to strongly bind to lipid membranes [6–12], in particular to anionic membranes. This is believed to be initiated by the three positive charges of the N-terminal region of hIAPP at neutral pH (N-terminus and the side chains of Lys_1 and Arg_{11}).

In vitro, hIAPP forms amyloid fibrils very fast and even at sub-micromolar protein concentrations [13]. This process is drastically accelerated in the presence of anionic membranes [6–12]. In contrast, progression of T2DM and most likely the in vivo deposition of pancreatic amyloid takes many years. Hence, some additional factors, such as chaperones or natively occurring inhibitory polypeptides, may act to prevent and/or clear amyloid deposits in vivo. In fact, a number of in vitro studies have shown that insulin is a potent inhibitor of hIAPP aggregation ([3,14] and refs. therein). In addition, the confinement of hIAPP in the tightly packed secretory granules has been also suggested to play an important role. In a recent computer simulation and theoretical study on a hIAPP fragment [15], we have put forward an explanation for the suppression of aggregation in

* Corresponding author.
E-mail address: roland.winter@tu-dortmund.de (R. Winter).

0301-4622/$ – see front matter © 2010 Elsevier B.V. All rights reserved.
doi:10.1016/j.bpc.2010.01.006

crowded cellular environments based on the statistical mechanics of aggregation phenomena in finite size systems. The observed effect may play a decisive role in hampering intracellular aggregation of highly insoluble amyloidogenic proteins, such as hIAPP, whereas aggregation may become unavoidable in the extracellular space. Of note, the mouse or rat variant of hIAPP (rat IAPP), which differs from hIAPP in only 6 out of the 37 residues, cannot form amyloid fibrils. However, it has been shown that both freshly dissolved mouse and human IAPP have a similar ability to insert into phospholipid monolayers [9,10].

The search for inhibitors of hIAPP aggregation is of high biomedical importance [16–19]. Natively occurring or rationally modified peptide sequences derived from short stretches of the amyloidogenic polypeptides which are important for self-association have been applied since several years by us and others to inhibit hIAPP amyloidogenesis [14,20,21]. An example of such a rationally designed, hIAPP-derived aggregation inhibitor is the hexapeptide NF(N-Me)GA(N-Me)IL (abbreviated NFGAIL-GI) [14,20,21] (see Fig. 1). NFGAIL-GI has been devised via the N-methylation of the backbone amides at G24 and I26 of the putative β-strand of the hIAPP amyloid core sequence hIAPP (22-27) or NFGAIL [22]. This low MW hexapeptide has been shown to bind with submicromolar affinity hIAPP and to attenuate its cytotoxic self-assembly and fibrillogenesis processes in bulk solutions [21]. However, it has been also shown that NFGAIL-GI was unable to affect an already started fibrillogenesis processes or to dissociate preformed amyloid fibrils [21]. A second example of a hIAPP-derived hIAPP aggregation inhibitor is the 37 residue polypeptide [(N-Me)G24, (N-Me)I26]-IAPP (abbreviated IAPP-GI) [16]. This is a conformationally constrained analog of full-length hIAPP which has been designed to mimic a non-amyloidogenic hIAPP conformer. This hIAPP analog contains instead of the hIAPP amyloid core sequence NFGAIL the N-methylated sequence NF(N-Me)GA(N-Me)IL while all other amino acid residues are the same as in full length hIAPP [16]. IAPP-GI has proven to be a highly soluble, non-amyloidogenic and non-cytotoxic hIAPP analog. Most importantly, IAPP-GI has been found to be able to bind hIAPP in bulk solution with low nanomolar affinity, to completely block its cytotoxic self-assembly and amyloidogenesis processes, and to redissociate already formed cytotoxic hIAPP oligomers and fibrils [16]. Most recently, IAPP-GI has also been shown to be a nanomolar-affinity inhibitor of insulin aggregation as well, and it has been suggested that interaction of early prefibrillar and non-toxic hIAPP and insulin species attenuates self-assembly and fibrillization of both insulin and hIAPP [17]. Spectroscopic analyses have indicated that the heterocomplexes have less α-helical content than insulin alone [17]. However, the effects of lipid membranes, which are highly abundant in the in vivo environment, on the above amyloid inhibitory peptide–peptide interactions are still largely unknown.

The goal of the presented study was to explore the amyloidogenic propensity and conformational properties of hIAPP in the presence of negatively charged membrane surfaces (DOPC/DOPG phospholipid bilayers) upon addition of the two hIAPP amyloid inhibitors IAPP-GI and NFGAIL-GI and to compare the effects of these two inhibitors to the effects of insulin, which is a natively occurring inhibitor of hIAPP fibrillogenesis, and rIAPP, which is a natively non-amyloidogenic IAPP analogue. In vivo, hIAPP aggregation may start and proceed at the water-cell membrane interface and anionic lipid membranes, which mimic cell membranes, have been shown to strongly enhance hIAPP fibrillization in vitro. As this process leads to membrane disintegration and cell degeneration, our studies should offer valuable information on the molecular mechanisms of hIAPP aggregation and cell degeneration and the inhibition of these processes by natively occurring or rationally designed compounds in a cell membrane-like environment [9–12]. To this end, attenuated total reflection Fourier-transform infrared (ATR-FTIR) spectroscopy was applied [18]. Owing to the exponentially decaying evanescent wave (penetration depth ~0.6 μm), only membrane-associated effects are recorded by this technique. Hence, the method allows determination of i) the adsorption of the peptides or their complexes at the lipid membrane, and ii) detection of fibrillization (β-sheet formation) at the water-lipid interface and/or within the lipid bilayer membrane. The data are compared with bulk spectroscopic data (in the absence of lipid membranes) on these systems employing CD spectroscopy and ThT fluorescence detection of amyloid formation [16,21].

2. Materials and methods

2.1. Materials

The peptides rIAPP, hIAPP(22–27) (NFGAIL) as well as the inhibitors NF(N-Me)GA(N-Me)IL (NFGAIL-GI) and [(N-Me)G24, (N-Me)I26]-IAPP (IAPP-GI) were synthesized and purified as described [21–23]. Deuterium oxide (D_2O), deuterium chloride (DCl), sodium dihydrogen phosphate (NaH_2PO_4), sodium hydrogen phosphate (Na_2HPO_4) and sodium chloride (NaCl) were from Sigma-Aldrich, St. Louis, MO, USA. Hexafluoro-2-propanol (HFIP) was from Fluka, trifluoroethanol (TFE) and chloroform from Merck. hIAPP was from Calbiochem (Lot## B77447, 70008), La Jolla, CA, USA. The lipids 1,2-dioleoyl-*sn*-glycero-3-phosphocholine (DOPC, zwitterionic) and 1,2-dioleoyl-*sn*-glycero-3-[phospho-*rac*-(1-glycerol)] (DOPG, anionic) were obtained from Avanti Polar Lipids, Alabaster, AL, USA.

2.2. Sample preparation

To avoid overlap with the amide-I' band of the peptides, D_2O was used instead of H_2O for the FTIR spectroscopic experiments. For all experiments, phosphate buffer (10 mM PO_4^{3-}, pD 7.4) in D_2O containing NaCl (total ionic strength: 100 mM) was used. Stock solutions of the lipids were prepared by dissolving a mixture of 7 mg DOPC and 3 mg DOPG in chloroform up to a concentration of 10 mg/mL. 50 μL (containing 0.5 mg of lipids) of this solution was dried under a stream of nitrogen. After evaporation of most of the chloroform, the samples were placed in a Speed-Vac for 3 h to remove residual solvent. Preparation of peptide solutions: 0.5 mg hIAPP (dry powder following lyophilization) was dissolved in 1 mL HFIP or TFE to yield a stock solution. 100 μL of the stock were dried overnight in a lyophilisator and dissolved in 1 mL buffer to yield a 10 μM solution. The designated peptide inhibitor was added to the buffer solution prior to the addition of hIAPP. To ensure interaction of the inhibitor with hIAPP, the solution was shaken for 3 h at room temperature using an overhead-shaker (20 rpm, Stuart Tube Rotator SB2, Barloworld Scientific Ltd., Staffordshire, UK). Preparation of large unilamellar vesicles: 0.5 mg of the DOPC/DOPG (7:3 w/w) — mixture were dissolved in 1 mL buffer and ultrasonicated for 10 min. After 5 circles of freezing and thawing, a homogeneous solution of multilamellar vesicles (MLV) was obtained. To yield a solution of large unilamellar vesicles (LUV), the dispersion was pressed 11 times through an extruder with a membrane filter made of polycarbonate (Avanti, pore diameter: 0.1 μm).

2.3. ATR-FTIR measurements

The ATR-FTIR measurements were performed using a Nicolet 6700 FTIR-Spectrometer equipped with a liquid nitrogen-cooled MCT-A detector (see schematics in Fig. 1b). The spectrometer chamber was continuously purged with dry air to remove water vapor. The ATR out-of-compartment accessory consists of a liquid jacketed Piketech ATR flow-through cell made of steel. A trapezoidal Ge-Crystal (Piketech, Madison, WI, 80 mm × 10 mm × 4 mm, angle of incidence: 45°) was used as internal reflection unit (IRE). Owing to the exponentially decaying evanescent wave with penetration depth of about 0.6 μm, only membrane-associated effects are visible and precipitation of aggregate in the sample is not an issue as it is in transmission experiments. A background spectrum was collected using the same

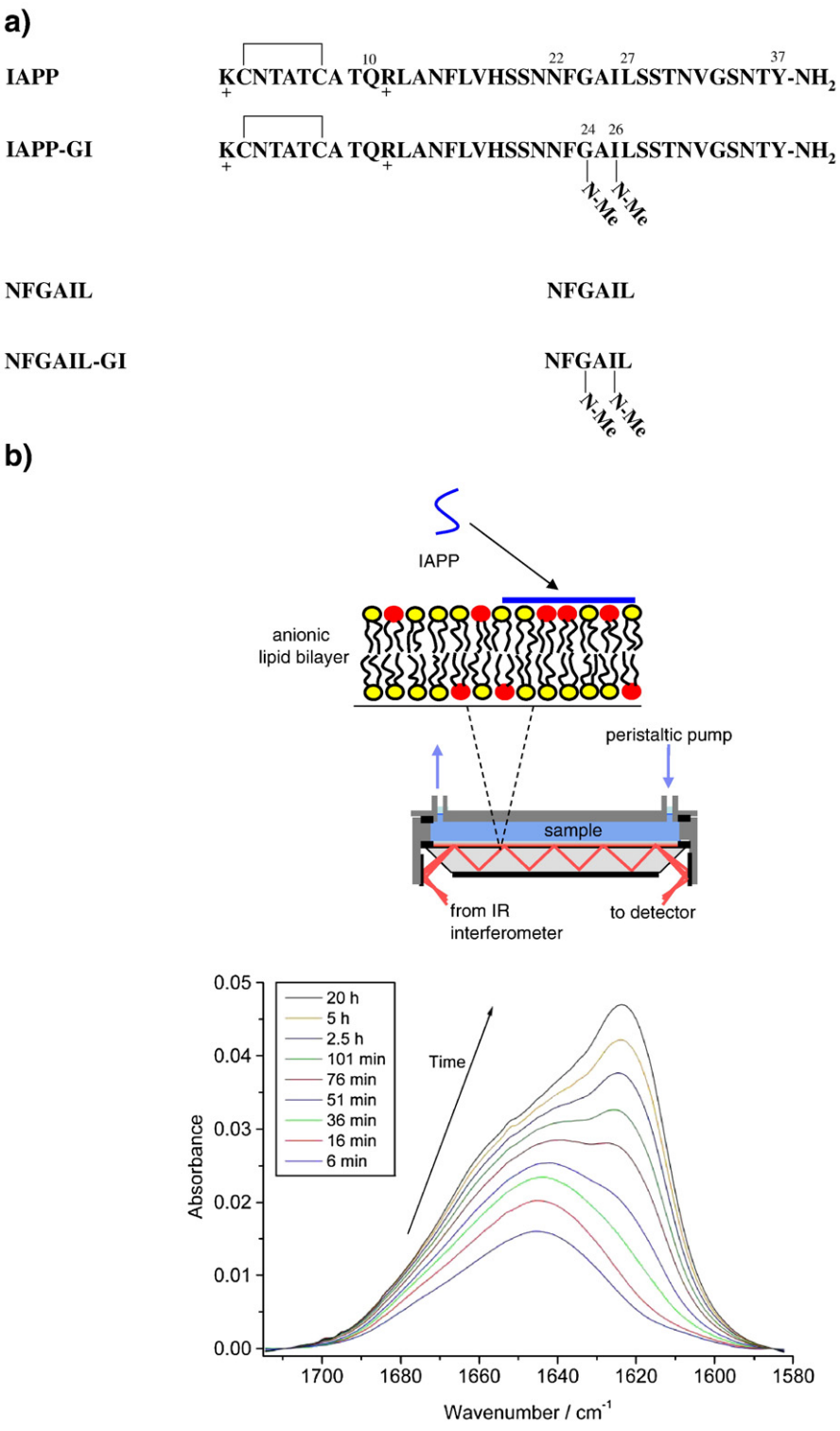

Fig. 1. a) Peptide sequence of the compounds used. b) Time course of the amide-I' band region of 10 μM hIAPP upon adsorption to the negatively charged DOPC/DOPG (7:3 w/w) membrane ($T = 25$ °C). At the top, a scheme of the ATR sample cell with an internal Ge reflection plate covered with the anionic lipid bilayer (red: DOPG, yellow: DOPC). IAPP molecules adsorbing to and aggregating at the membrane are detected while those distant from the membrane are merely visible owing to the low penetration depth of the evanescent IR wave [18].

IRE before the sample measurements. Typically, spectra of 128 scans were measured with a resolution of 2 cm^{-1}. The measurements were performed at 25 °C. Processing of the spectra was performed using GRAMS (Thermo Electron). After subtraction of the lipid background together with the buffer, the spectra were baseline corrected between 1710 and 1585 cm^{-1} and offset corrected. Data analysis and band assignment has been performed as described before [18,24–28]. No smoothing has been applied to any of the spectra.

The freshly prepared solution of large unilamellar vesicles (LUVs) was carefully injected into the ATR-flow-cell, which was maintained at 25 °C. Spreading of the vesicles takes place spontaneously. After adsorption over night, the membrane was washed with buffer over a

time period of 6 h. For this purpose, 2 mL of buffer was pumped from a reservoir into the sample compartment (at a rate of 1.4 mL/min). Lipids which are not strongly adhering to the crystal surface are dissolved in the washing liquid. Adsorption of the membrane was followed by detecting the band intensity of the lipid-bands over time. To ensure the integrity of the membrane, the hIAPP solution was injected into the ATR-cell by means of the peristaltic pump at 1.4 mL/min. Changes in amide-I'-band intensity were recorded over time. Spectra were collected every 5 min for a time period of 20 h.

For the measurements of the pure inhibitors, a solution of 10 μM rIAPP, IAPP-GI, NFGAIL-GI, or NFGAIL was injected into the membrane-containing ATR cell as in the previous experiment. Spectra were collected every 5 min for a time period of 20 h. Inhibition with rIAPP: 10 μM hIAPP was added to 10 μM rIAPP. The sample was shaken for 3 h at room temperature in an overhead-shaker. Inhibition with insulin: Insulin was dissolved in D_2O at pH 3.5 to obtain a 10 μM solution. NaCl and Na_2HPO_4 were added resulting in a 10 mM PO_4^{3-} buffer solution with a total ionic strength of 100 mM. The pH was adjusted to 7.4. hIAPP was dissolved in the insulin solution to finally obtain a solution of 10 μM hIAPP and 10 μM insulin. Inhibition with IAPP-GI: 10 μM hIAPP was added to 10 μM IAPP-GI. Inhibition with NFGAIL-GI: Before uptake of hIAPP, the freeze-dried NFGAIL was dissolved in 1 mL buffer. 10 μM hIAPP was added to 10 or 100 μM NFGAIL-GI. The mixtures were shaken for 3 h at room temperature in an overhead-shaker. Redissolving of aggregated hIAPP by means of IAPP-GI or NFGAIL-GI: 10 μM hIAPP was injected into the membrane containing cell and allowed to adsorb and aggregate for 20 h. Then, a solution of 10 μM IAPP-GI was injected by means of the peristaltic pump. The same experiment was performed with 100 μM IAPP-GI, and 10 or 100 μM NFGAIL-GI.

3. Results and discussion

3.1. Conformational changes of hIAPP in the presence of negatively charged (DOPC/DOPG) lipid membranes as revealed by ATR-FTIR spectroscopy

First we studied the conformational changes of pure hIAPP in the presence of the DOPC/DOPG (7:3 w/w) lipid bilayer at 25 °C. To evaluate the changes in secondary structure of hIAPP at the membrane interface, we collected FTIR-spectra up to 20 h in intervals of 5 min after the injection of a solution of 10 μM hIAPP into the ATR cell containing the spread anionic lipid bilayer film. Due to interfacial adsorption, the local concentration close to the lipid bilayer interface increases with time, *t*, and aggregation is induced. During the aggregation process, the peak maximum of the amide-I' band of hIAPP shifts from 1645 cm^{-1} towards 1624 cm^{-1}, indicating a decrease of unordered structures and a concomitant increase of β-structures [18,26,28,29]. In Fig. 1, ATR-FTIR spectra for selected time points are presented. The data clearly show that aggregation occurs at the membraneous interface beyond about 16 min. A quantitative decomposition of the amide-I' band region into subbands using Fourier self-deconvolution and 2nd derivative of the normalized spectra [18,24–26] reveals distinct bands for the initial hIAPP conformation at about 1674, 1666, 1662, 1652, 1645 and 1638 cm^{-1}, with the most prominent band at 1645 cm^{-1} (see Table 1). Assuming similar transition dipole moments for the various conformers, an initial population of about 29% turns and loops, 17% α-helices, 32% β-sheets and 22% unordered conformations can be determined (accuracy ~3%). During the aggregation process, bands at ~1684, 1626 and 1619 cm^{-1} appear. The strong bands at 1619 and 1626 cm^{-1} indicate the presence of intermolecular β-sheets (~39-43%) with strong hydrogen bonding [18,24–26]. Intermolecular β-sheet formation occurs at the expense of a decrease of turns/loops, α-helical and unordered structures of hIAPP [13,29,30]. According to Engel et al., the growth of fibrils in the lipid membrane rather than the actual presence of fibrils probably leads to membrane disruption [12].

3.2. Effect of the hIAPP-derived peptides and insulin on hIAPP fibrillization at the lipid interface

To study the effect of the peptide inhibitors and to determine their relative potencies in suppressing the fibrillation process of hIAPP in the membraneous context, peptides and their mixtures with hIAPP were investigated by ATR-FTIR-spectroscopy in the presence of the solid-supported lipid membrane. After injection of the peptide solutions into the membrane containing cell, FTIR spectra were collected each 5 min for a time period of 20 h.

Fig. 2 exhibits a collection of spectra after an incubation time of 20 h. The spectra were not normalized, so the magnitude of interaction with the membrane corresponds to the intensity of the amide-I' band. The shift of the peak maximum of hIAPP from ~1645 cm^{-1} towards lower wavenumbers (~1625 cm^{-1}) indicates aggregation and amyloid formation via (parallel) intermolecular β-sheet formation [24,28,29]. In addition, results shown in Fig. 2a suggest that the non-amyloidogenic rIAPP is strongly interacting with the anionic membrane, but without formation of amyloid fibrils. The peak maximum of adsorbed rIAPP appears at 1647 cm^{-1}, which is consistent with a largely disordered/α-helical conformation of rIAPP when inserted into the lipid bilayer as suggested by previous reports [8–10]. Differences in conformational properties of unaggregated hIAPP and membrane-adsorbed rIAPP seem to be small. Populations of about 28% turns and loops, 13% α-helices, 43% intramolecular β-sheets and 16% unordered conformations are determined for the membrane-adsorbed rIAPP.

The spectrum of IAPP-GI exhibits a broad amide I peak around 1643 cm^{-1}, which is characteristic of a large contribution of random conformations. The high peak intensity points to a significant interaction of IAPP-GI with the lipid interface. Differences in conformational properties of adsorbed hIAPP immediately after the beginning of the incubation process and IAPP-GI are also small [27]. The amide-I' band maximum shifts from about 1646 to 1644 cm^{-1}. Quantitative analysis reveals a population of about 31% turns and loops, 14% α-helical, 40% β-sheet and 16% unordered conformations for IAPP-GI. Thus, the structural characteristics of membrane bound IAPP-GI appears to be very similar to those of membrane-bound rIAPP. In strong contrast to these findings, no significant amide-I' band intensities are observed for NFGAIL-GI and NFGAIL, i.e. these peptides are not interacting with the anionic lipid bilayer membrane at all, probably due to the lack of the N-terminal sequence of hIAPP, which is believed to be largely responsible for the hIAPP interaction with the lipid membrane [9,10]. In the case of NFGAIL, strong aggregation and amyloidogenesis have been observed in the bulk phase, whereas NFGAIL-GI has been shown to be a highly soluble and non-amyloidogenic peptide [20–22].

Fig. 2b shows the corresponding ATR-FTIR spectra of the 1:1 (mol:mol) mixtures of IAPP-GI, NFGAIL-GI, rIAPP, and insulin with hIAPP as well as the spectra of hIAPP alone in the presence of the anionic membrane. As stated before, ATR-FTIR probes the immediate environment above the membrane. The peptide mixtures were shaken

Table 1
Secondary structure analysis of different IAPP species (accuracy ca. 5%) (see also [29]).

Secondary structure element (wavenumber assignment)	Secondary structure content			
	hIAPP (bulk)	hIAPP (adsorbed)	rIAPP (adsorbed)	IAPP-GI (adsorbed)
Turns and loops (~1684, 1674, 1666, 1662 cm^{-1})	~29%	~21%	~28%	~31%
α-Helices (~1652 cm^{-1})	~17%	~11%	~13%	~14%
Unordered structures (~1645 cm^{-1})	~22%	~11%	~16%	~16%
Intramolecular β-sheets (~1638 cm^{-1})	~32%	~13%	~43%	~40%
Intermolecular β-sheets (~1626, 1619 cm^{-1})	–	~43%	–	–

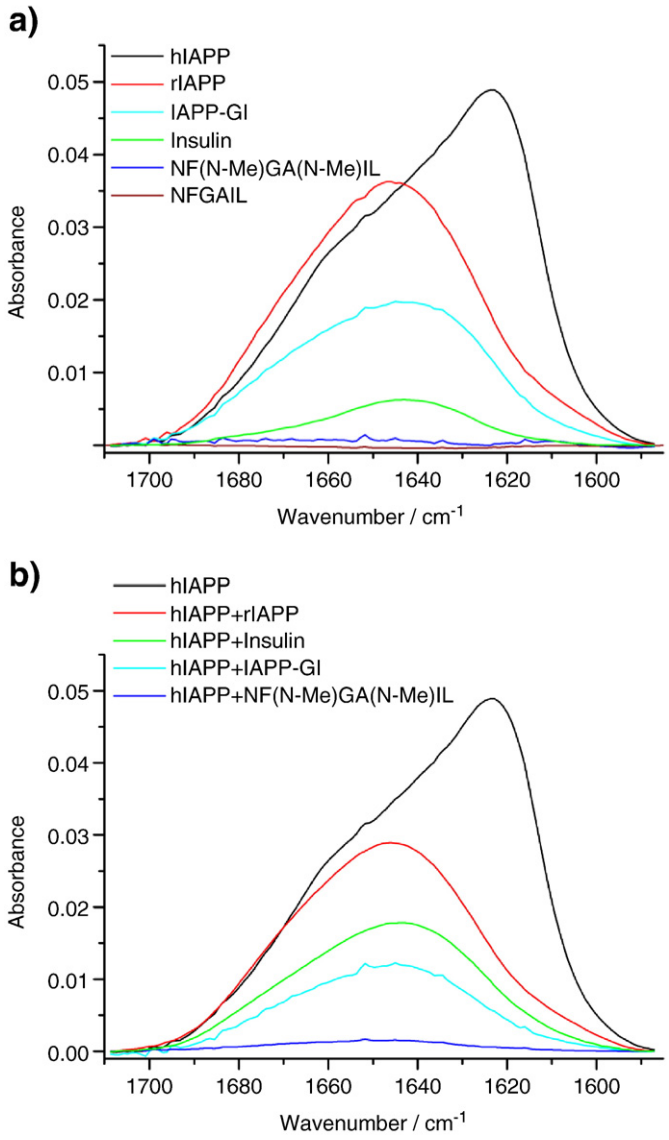

Fig. 2. Comparison of the amide-I' bands of amyloidogenic hIAPP and different peptide inhibitors (a) with those of (1/1) mixtures of peptide inhibitors (rIAPP, insulin, IAPP-GI, NFGAIL-GI with hIAPP (b) after 20 h of incubation in contact with the lipid bilayer DOPC/DOPG (7:3 w/w).

for 3 h at room temperature before the samples were injected into the ATR unit. Clearly, for all these mixtures no intermolecular β-sheet and amyloid formation at the membraneous interface is observed. In the case of IAPP-GI, insulin, and rIAPP, we can conclude that these peptides strongly inhibit hIAPP aggregation and fibrillization. However, their hetero-complexes with hIAPP are still able to interact/adsorb at the lipid membrane, albeit to a lesser extent than the components alone. A possible reason for this finding might be that the N-terminal sequence of hIAPP, which partitions into the lipid bilayer membrane, is not completely blocked by the hetero-complex formation with the peptides. Comparison of the FTIR spectra of the peptide components alone with the spectra of the hIAPP-peptide mixtures reveals that upon hetero-complex formation, no marked conformational changes occur (Figs. 1 and 2).

Surprisingly, the 6-residue peptide NFGAIL-GI proved to be the most potent inhibitor with regard to both inhibiting hIAPP fibrillogenesis and hIAPP interaction with the lipid membrane. No adsorption at the lipid interface was observed for the hIAPP-NFGAIL-GI mixture in the ATR-FTIR spectra. Hence we can conclude that the observed strong inhibitory effect of the NFGAIL-GI on hIAPP fibrillization at the lipid interface is due to formation of non-amyloidogenic hIAPP-NFGAIL-GI hetero-complexes — likely in the aqueous phase — which are completely unable to interact with, or adsorb at, the lipid membrane.

3.3. Studies on the effect of IAPP-GI and NFGAIL-GI on preformed and membrane-embedded hIAPP amyloid fibers

In previous studies it has been shown that IAPP-GI dissociates cytotoxic hIAPP oligomers and fibrils formed in bulk solution and that it is thus able to reverse their cytotoxic effects [16]. To address the question whether IAPP-GI can also dissociate hIAPP aggregates and fibrils which form in the presence of anionic lipid membranes and become embedded in the membrane, we injected IAPP-GI at an 1/1 (10 μM) or 10/1 (100 μM) molar ratio to hIAPP monomers into the ATR-cell which contained hIAPP (10 μM) already aggregated at the lipid interface. In addition, the effect of NFGAIL-GI on pre-formed hIAPP fibrils at a 1/1 or 10/1 ratio to hIAPP was also studied. Of note, NFGAIL-GI was previously reported to be unable to redissociate hIAPP fibrils in bulk solution [21]. ATR-FTIR-spectra were collected for a time period of 4 (for the 1/1 inhibitor/IAPP ratio) or 7 days (for the 10/1 ratio).

As shown in Fig. 3a and c, no decrease in the intensity of the aggregation band of hIAPP was observed in the presence of both IAPP-GI and NFGAIL-GI at the 1/1 molar ratio. At the time point of 100 h, even a further increase of the aggregation band intensity was observed at the lipid interface as compared to the band obtained at 20 h. Addition of a 10-fold excess (100 μM) of the inhibitors to already aggregated hIAPP results in a large increase of the amide-I' band intensity in case of IAPP-GI (Fig. 3b), whereas no changes are observed in the case of NFGAIL-GI (Fig. 3d). This observation can be rationalized by the contribution of IAPP-GI to the intensity of the amide-I' band, whereas NFGAIL-GI does not adsorb to the lipid interface and hence is not detected by the ATR evanescent wave. The poor interaction of NFGAIL-GI with the lipid interface was confirmed by ATR-FTIR spectroscopy of the pure component in the presence of the lipid membrane (see Fig. 2, bottom). Hence, we can conclude that the NFGAIL-GI is unable to redissolve preformed hIAPP amyloid aggregates that form in the presence of the lipid membrane.

IAPP-GI was found to be able to adsorb at the lipid bilayer, which results in a marked contribution to the amide-I' band on top of the amide-I' band intensity originating from the hIAPP amyloid fibrils. In Fig. 3c, the peak maximum of the amide-I' band is seen to shift from 1620 to 1626 cm^{-1}, and the amyloid β-sheet content seems to decrease in favor of unordered secondary structure content. As seen in Fig. 4, subtraction of the amyloid hIAPP contribution (red curve in Fig. 3c, addition of IAPP-GI at $t=0$) reveals that a broad band is remaining around 1640–1645 cm^{-1}. Its intensity increases with time, indicating an increasing adsorption of mainly unordered IAPP-GI. Notably, the peak maximum shifts still slightly towards smaller wavenumbers, which is probably due to a further slight increase of hIAPP aggregation. Hence, the ability of IAPP-GI to redissolve hIAPP amyloid, which is observed in bulk solution, is lost when the amyloid aggregates form in the presence of lipids. Possible reasons accounting for this finding may be (a) that IAPP-GI becomes immobilized by its N-terminus in the lipid matrix and is thus unable to interact with hIAPP amyloid and/or (b) that, in contrast to the events observed in bulk, the interaction of hIAPP amyloid fibrils with IAPP-GI might be prohibited by the strong and rigid embedding of hIAPP fibrils in the lipid membrane. This latter explanation would be consistent with recent results from spectroscopic and fluorescence microscopic studies [9,12].

4. Conclusions

Here we tested whether recently reported inhibitors of hIAPP fibrillogenesis in bulk including the two rationally designed hIAPP-derived inhibitors IAPP-GI and NFGAIL-GI, the natively occurring IAPP

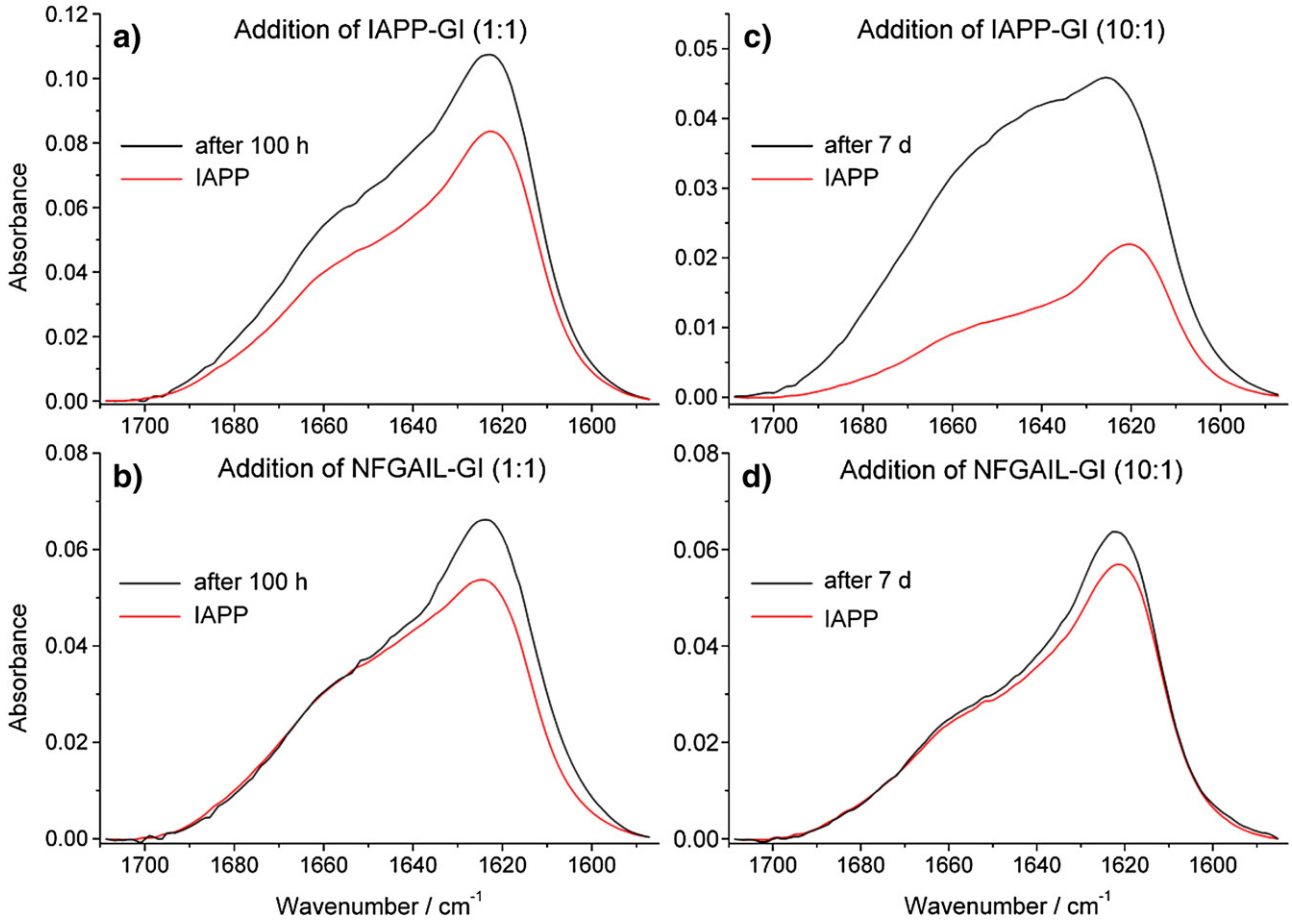

Fig. 3. Amide-I' band of hIAPP after 20 h of incubation at the lipid membrane (red curves). Left (black curves): 100 h of incubation with a) (1/1) IAPP-GI or b) (1/1) NFGAIL-GI. Right (black curves): 7 d of incubation with c) 10-fold excess of IAPP-GI or d) 10-fold excess of NFGAIL-GI.

amyloidogenesis inhibitor insulin, and the natively non-amyloidogenic IAPP analog rIAPP are also able to inhibit hIAPP amyloidogenesis in the presence of anionic lipid membranes. Such membraneous interfaces have been shown to strongly accelerate formation of hIAPP fibrils and this process has been causally linked to membrane damage

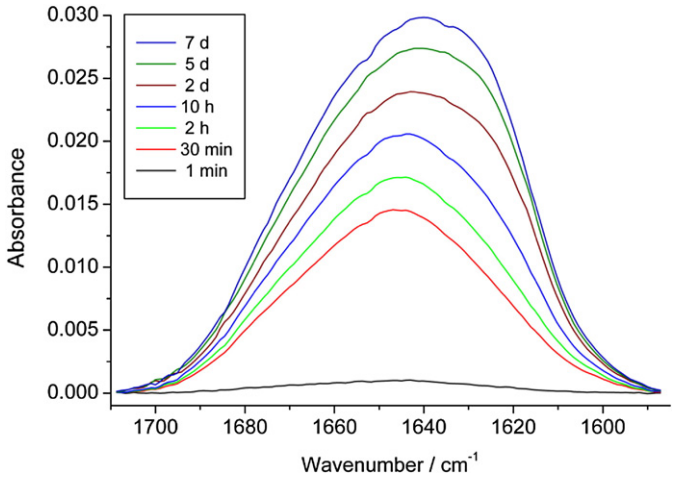

Fig. 4. ATR-FTIR spectra of IAPP-GI, which was added as peptide inhibitor into the ATR-flow-cell, where hIAPP was allowed to pre-aggregate for 20 h in the presence of the anionic membrane. The contribution of aggregated hIAPP was then subtracted from the amide-I' band of the hIAPP-IAPP-GI mixture. Selected spectra over a time course of 7 days are shown.

[9–12]. Our results show that the 37-residue non-amyloidogenic hIAPP mimic IAPP-GI as well as the N-methylated hexapeptide NFGAIL-GI have strong inhibitory effects on in vitro hIAPP fibrillization at the membraneous interface, suggesting that these peptides may be able to suppress pathogenic self-association of hIAPP also in vivo. Insulin and rIAPP are also found to inhibit hIAPP fibrillization (Fig. 5). Importantly, interactions of IAPP-GI, rIAPP, and insulin with hIAPP weakened but did not strongly affect hIAPP-membrane interaction, whereas interaction of NFGAIL-GI with hIAPP completely blocked hIAPP-membrane interaction. Our results suggest that the inhibitory effects of IAPP-GI, rIAPP, and insulin on IAPP fibrillogenesis at the water-membrane interface are due to formation of non-amyloidogenic hetero-complexes with hIAPP, likely in the bulk aqueous phase, which are still able to adsorb at the membrane but unable to damage it [17,23]. By contrast, a mechanism of hIAPP sequestration due to formation of non-amyloidogenic hIAPP-NFGAIL-GI hetero-complexes in the aqueous phase appears to account for the observed strong inhibitory effect of NFGAIL-GI on hIAPP fibrillization [21]. Finally, our studies also showed that once hIAPP was fibrillized and thus embedded in the lipid membrane, no fibril disaggregation could be achieved by all tested hIAPP amyloid inhibitors.

It has been recently reported that IAPP-GI is also able to bind with low nanomolar affinity the β-amyloid peptide (Aβ) of the Alzheimer's disease and to completely inhibit its cytotoxic self-assembly and fibrillogenesis processes in bulk solution [17]. Given the fact that the lipid membrane-water environment also strongly affects Aβ aggregation, it would now be very interesting to test whether IAPP-GI is also able to block Aβ aggregation in the presence of lipids.

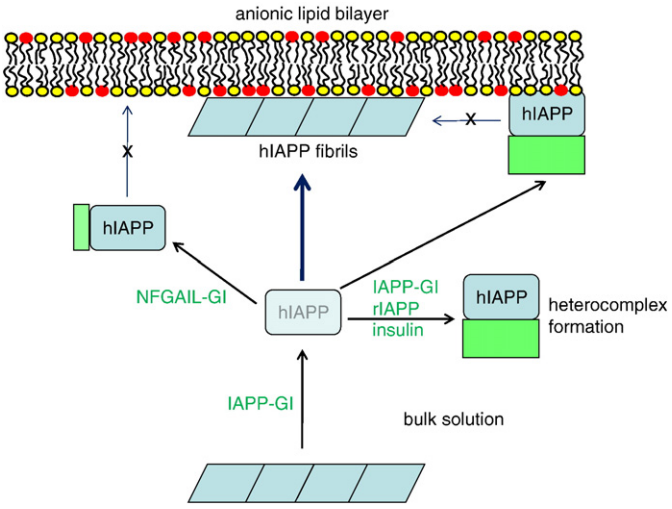

Fig. 5. Proposed mechanism of interaction of hIAPP with anionic lipid bilayers in the absence and presence of insulin, rIAPP, and the peptide inhibitors IAPP-GI and NFGAIL-GI. IAPP-GI as well as the N-methylated hexapeptide NFGAIL-GI are found to exert strong inhibitory effects on hIAPP fibrillization at the membraneous interface (and in bulk as shown previously [21,23]) while insulin and rIAPP are also found to inhibit hIAPP fibrillization. Interactions of IAPP-GI, rIAPP, and insulin with hIAPP in the bulk results in formation of heterocomplexes [17,21,23] which strongly affect hIAPP-membrane interaction and hIAPP β-sheet formation and fibrillogenesis at the membraneous interface, albeit adsorption of the heterocomplexes at the membrane may still occur. Interaction of NFGAIL-GI with hIAPP in the bulk results in heterocomplexes [21] which seem to completely inhibit hIAPP-membrane interaction and thus they block hIAPP fibrillogenesis at the membrane. Neither hIAPP-GI nor NFGAIL-GI are able to cause dissociation of preformed hIAPP fibrils which are embedded in the lipid membrane. For comparison, hIAPP-GI has been recently shown to be able to dissociate already formed hIAPP fibrils in the bulk while NFGAIL-GI was unable to do so [21,23].

Acknowledgements

Financial support from the Deutsche Forschungsgemeinschaft to AK and RW is gratefully acknowledged. We thank Marianna-Tatarek-Nossol for HPLC purifications of the hIAPP-derived inhibitors and rIAPP and Erika Andreetto for synthesis of IAPP-GI and rIAPP.

References

[1] R.L. Hull, G.T. Westermark, P. Westermark, S.E. Kahn, Islet amyloid: a critical entity in the pathogenesis of type 2 diabetes, J. Clin. Endocrinol. Metab. 89 (2004) 3629–3643.
[2] S.E. Kahn, D.A. D'Alessio, M.W. Schwartz, W.Y. Fujimoto, J.W. Ensinck, G.J. Taborsky, D. Porte, Evidence of cosecretion of islet amyloid polypeptide and insulin by β-cells, Diabetes 39 (1990) 634–638.
[3] J.D. Knight, J.A. Williamson, A.D. Miranker, Interaction of membrane-bound islet amyloid polypeptide with soluble and crystalline insulin, Protein Sci. 17 (2008) 1–7.
[4] P.A. Rushing, M.M. Hagen, R.J. Seeley, T.A. Lutz, D.A. D'Alessio, E.L. Air, S.C. Woods, Inhibition of central amylin signaling increase food intake and body adiposity in rats, Endocrinology 142 (2001) 5035–5038.
[5] S. Grudzielanek, V. Smirnovas, R. Winter, The effects of various membrane physical-chemical properties on the aggregation kinetics of insulin, Chem. Phys. Lipids 149 (2007) 28–39.
[6] J.D. Knight, A.D. Miranker, Phospholipid catalysis of diabetic amyloid assembly, J. Mol. Biol. 341 (2004) 1175–1187.
[7] S.A. Jayasinghe, R. Langen, Lipid membranes modulate the structure of islet amyloid polypeptide, Biochemistry 44 (2005) 12113–12119.
[8] J.D. Knight, J.A. Hebda, A.D. Miranker, Conserved and cooperative assembly of membrane-bound α-helical states of islet amyloid polypeptide, Biochemistry 45 (2006) 9496–9508.
[9] M.F.M. Engel, H. Yigittop, R.C. Elgersma, D.T.S. Rijkers, R.M.J. Liskamp, B. de Kruiff, J.W.M. Höppener, J.A. Killian, Islet amyloid polypeptide inserts into phospholipid monolayers as monomer, J. Mol. Biol. 356 (2006) 783–789.
[10] D.H.J. Lopes, A. Meister, A. Gohlke, A. Hauser, A. Blume, R. Winter, Mechanism of islet amyloid polypeptide fibrillation at lipid interfaces studied by infrared reflection absorption spectroscopy, Biophys. J. 93 (2007) 3132–3141.
[11] Y.A. Domanov, P.K.J. Kinnunen, Islet amyloid polypeptide forms rigid lipid-protein amyloid fibrils on supported phospholipid bilayers, J. Mol. Biol. 376 (2008) 42–54.
[12] F.M. Maarten, L.K. Engel, C.C. Kleijer, H.J.D. Meeldijk, J. Jacobs, A.J. Verkleij, B. de Kruijff, J.A. Killian, J.W.M. Höppener, Membrane damage by human islet amyloid polypeptide through fibril growth at the membrane, Proc. Natl Acad. Sci. USA 105 (2008) 6033–6038.
[13] R. Kayed, J. Bernhagen, N. Greenfield, K. Sweimeh, H. Brummer, W. Voelter, A. Kapurniotu, Conformational transitions of islet amyloid polypeptide (IAPP) in amyloid formation *in vitro*, J. Mol. Biol. 287 (1999) 781–796.
[14] S. Gilead, H. Wolfenson, E. Gazit, Molecular mapping of the recognition interface between the islet amyloid polypeptide and insulin, Angew. Chem. Int. Ed. 45 (2006) 6476–6480.
[15] G. Singh, I. Brovchenko, A. Oleinikova, R. Winter, Peptide aggregation in finite systems, Biophys. J. 95 (2008) 3208–3221.
[16] L.-M. Yan, A. Velkova, M. Tatarek-Nossol, E. Andreetto, A. Kapurniotu, IAPP mimic blocks Aβ cytotoxic self-assembly: cross-suppression of amyloid toxicity of Aβ and IAPP suggests a molecular link between Alzheimer's disease and type II diabetes, Angew. Chem. Int. Ed. 46 (2007) 1246–1252.
[17] A. Velkova, M. Tatarek-Nossol, E. Andreetto, A. Kapurniotu, Exploiting cross-amyloid interactions to inhibit protein aggregation but not function: nanomolar affinity inhibition of insulin aggregation by an IAPP mimic, Angew. Chem. Int. Ed. 47 (2008) 7114–7118.
[18] R. Mishra, B. Bulic, D. Sellin, S. Jha, H. Waldmann, R. Winter, Small-molecule inhibitors of islet amyloid polypeptide fibril formation, Angew. Chem. Int. Ed. 47 (2008) 4679–4682.
[19] A. Kapurniotu, Amyloidogenicity and cytotoxicity of islet amyloid polypeptide, Biopolymers 60 (2001) 438–459.
[20] A. Kapurniotu, A. Schmauder, K. Tenidis, Structure-based design and study of non-amyloidogenic, double N-methylated IAPP amyloid core sequences as inhibitors of IAPP amyloid formation and cytotoxicity, J. Mol. Biol. 315 (2002) 339–350.
[21] M. Tatarek-Nossol, L.-M. Yan, A. Schmauder, K. Tenidis, G. Westermark, A. Kapurniotu, Inhibition of hIAPP amyloid-fibril formation and apoptotic cell death by a designed hIAPP amyloid-core-containing hexapeptide, Chem. Biol. 12 (2005) 797–809.
[22] K. Tenidis, M. Waldner, J. Bernhagen, W. Fischle, M. Bergmann, M. Weber, M.-L. Merkle, W. Voelter, H. Brunner, A. Kapurniotu, Identification of a penta- and hexapeptide of islet amyloid polypeptide (IAPP) with amyloidogenic and cytotoxic properties, J. Mol. Biol. 295 (2000) 1055–1071.
[23] M.-L. Yan, M. Tatarek-Nossol, A. Velkova, A. Kazantzis, A. Kapurniotu, Design of a mimic of nonamyloidogenic and bioactive human islet amyloid polypeptide (IAPP) as nanomolar affinity inhibitor of IAPP cytotoxic fibrillogenesis, Proc. Natl Acad. Sci. USA 103 (2006) 2046–2051.
[24] S. Grudzielanek, V. Smirnovas, R. Winter, Solvation-assisted pressure tuning of insulin fibrillation: from novel aggregation pathways to biotechnological applications, J. Mol. Biol. 356 (2006) 497–509.
[25] Y. Cordeiro, J. Kraineva, M.C. Suarez, A.G. Tempesta, J.W. Kelly, J.L. Silva, R. Winter, D. Foguel, Fourier transform infared spectroscopy provides a fingerprint for the tetramer and for the aggregates of transthyretin, Biophys. J. 91 (2006) 957–967.
[26] D. Radovan, V. Smirnovas, R. Winter, Effect of pressure on islet amyloid polypeptide aggregation: revealing the polymorphic nature of fibrillation process, Biochemistry 47 (2008) 6352–6360.
[27] M. Zein, R. Winter, Effect of temperature, pressure and lipid acyl-chain length on the structure and phase behaviour of phospholipid-gramicidin bilayers, Phys. Chem. Chem. Phys. 2 (2000) 4545–4551.
[28] W. Dzwolak, S. Grudzielanek, V. Smirnovas, R. Ravindra, C. Nicolini, R. Jansen, A. Loksztejn, S. Porowski, R. Winter, Ethanol-perturbed amyloidogenic self-assembly of insulin: looking for origins of amyloid strains, Biochemistry 44 (2005) 8948–8958.
[29] S. Jha, D. Sellin, R. Seidel, R. Winter, R. Amyloidogenic, propensities and conformational properties of ProIAPP and IAPP in the presence of lipid bilayer membranes, J. Mol. Biol. 389 (2009) 907–920.
[30] F. Evers, C. Jeworrek, S. Tiemeyer, K. Weise, D. Sellin, M. Paulus, B. Struth, M. Tolan, R. Winter, Elucidating the mechanism of lipid membrane-induced IAPP fibrillogenesis and its inhibition by the red wine compound resveratrol. A synchrotron x-ray reflectivity study, J. Am. Chem. Soc. 131 (2009) 9516–9521.